Available online at www.sciencedirect.com
SCIENCE DIRECT®
Journal of Solid State Chemistry 172 (2003) 27–34
JOURNAL OF SOLID STATE CHEMISTRY
http://elsevier.com/locate/jssc

The ternary rare earth ruthenium gallides $R_3Ru_4Ga_{15}$ (R = Y, Tb–Er) with a new structure type, a further example of a recently recognized large family of structures

Martin Schlüter and Wolfgang Jeitschko*

Institut für Anorganische und Analytische Chemie, Westfälische Wilhelms-Universität Münster, Wilhelm Klemm-Strasse 8, D-48149 Münster, Germany

Received 20 May 2002; received in revised form 21 August 2002

Abstract

The title compounds were prepared by reaction of the elemental components at high temperature. They crystallize with a new orthorhombic structure type which was determined from single-crystal diffractometer data of $Ho_3Ru_4Ga_{15}$: *Pnma*, $a = 871.7(1)$ pm, $b = 956.4(1)$ pm, $c = 1765.9(3)$ pm, $Z = 4$, $R = 0.040$ for 1039 structure factors and 114 variable parameters. The structure may be viewed as consisting of two kinds of atomic layers, although atomic bonding within and between the layers is comparable strength, as can be judged from the near-neighbor environments, where all of the 15 atomic sites have high coordination numbers. One kind of atomic layers (*A*) contains all of the holmium and additional gallium atoms in the ratio Ho:Ga = 3:5 with a unit mesh content of $2Ho_3Ga_5$; these layers are flat. The other layers (*B*) consist of sheets of corner- and edge-sharing condensed $RuGa_6$ octahedra, which are extremely compressed resulting in a hexagonal close-packed, puckered net with a Ru:Ga ratio of 2:5 and a unit mesh content of $4Ru_2Ga_5$. These nets alternate in the sequence *ABAB*, *ABAB*, thus yielding the formula $4Ho_3Ga_5 \cdot 8Ru_2Ga_5 = 4Ho_3Ru_4Ga_{15}$. Similar layers are observed in the structures of $Y_2Co_3Ga_9$, $Gd_3Ru_4Al_{12}$, $Er_4Pt_9Al_{24}$, $CeOsGa_4$, $CaCr_2Al_{10}$, and the four stacking variants with the compositions $TbRe_2Al_{10}$, $DyRe_2Al_{10}$, $YbFe_2Al_{10}$, and $LuRe_2Al_{10}$.

1. Introduction

In the course of our investigations of ternary intermetallics of the rare earth (*R*) and transition metals (*T*) with a high content of gallium we have reported on the series $R_2Ru_3Ga_9$ [1] with $Y_2Co_3Ga_9$-type structure [2], the series $R_2Ru_3Ga_{10}$ [3] with a new structure type, and RRu_2Ga_8 [3] with $CaCo_2Al_8$-type structure [4]. With osmium as transition metal component we have found the series $ROsGa_3$ [5] with $TmRuGa_3$-type structure [6] and $ROsGa_4$ with a new structure type determined for $CeOsGa_4$ [5]. Here we communicate our results on another series of rare earth ruthenium gallides with the composition $R_3Ru_4Ga_{15}$. The crystal structures of these ternary compounds with a high content of gallium may frequently be viewed as consisting of atomic layers of two kinds. One kind contains all of the rare earth and some gallium atoms; the other layers contain the remaining gallium and all of the transition metal atoms. Similar atomic layers have been found in several series of ternary aluminides. In this article we give a brief review of these compounds. Some results of our investigations on the series $R_3Ru_4Ga_{15}$ have already been presented at a conference [7], but are reported in full here for the first time.

2. Sample preparation and lattice constants

The compounds were prepared from the elemental components, all with nominal purities >99.9%. The rare earth elements were purchased in the form of ingots; they were cut to pieces prior to the cold-pressing. Ruthenium (Degussa) was obtained in powder form and gallium (VAW) in the form of ingots which were crushed to small pieces at liquid nitrogen temperature. The three components with a total weight of ca. 0.5 g were mixed in the ratio *R*:Ru:Ga = 1:1:10. The buttons were arc-melted at least two times to improve the homogeneity of the sample. The single crystals of $Ho_3Ru_4Ga_{15}$ used for the structure determination were

*Corresponding author. fax: +251-8333-136.
E-mail address: jeitsch@uni-muenster.de (W. Jeitschko).

0022-4596/03/$ - see front matter © 2003 Elsevier Science (USA). All rights reserved.
doi:10.1016/S0022-4596(02)00043-9

isolated from a sample that had been annealed in a water-cooled silica tube in a high-frequency furnace for 3 h just below the (visually observable but unknown) melting point. The excess rare earth and gallium in the samples were dissolved in diluted hydrochloric acid, which attacks the crystals of the ternary compounds at a much lower rate.

All of these ternary gallides are stable on air for long periods and show silvery metallic luster. The powders are dark gray. Energy-dispersive X-ray fluorescence analyses in a scanning electron microscope did not reveal any impurity elements heavier than sodium.

Guinier powder diagrams of the new intermetallic compounds were recorded with monochromated Cu$K\alpha_1$ radiation and α-quartz ($a = 491.30$ pm, $c = 540.46$ pm) as an internal standard. To ensure proper assignment of the indices the observed patterns were compared with the ones calculated [8] assuming the atomic positions resulting from the structure determination of the holmium compound. The lattice constants (Table 1) were obtained by least-squares fits. The cell volumes of the compounds are plotted in Fig. 1.

3. Crystal structure of $Ho_3Ru_4Ga_{15}$

A single crystal of the holmium compound was selected for the structure determination on the basis of Laue patterns. X-ray intensity data were recorded on an Enraf–Nonius four-circle diffractometer (CAD4) using graphite-monochromated MoKα radiation, a scintillation counter with pulse height discrimination, and background counts at both ends of each $\theta/2\theta$ scan. A correction for absorption was made on the basis of psi scan data. It should be mentioned that the orthorhombic unit cell found first (for a crystal of the isotypic terbium compound) was too small. The structure determination resulted in a disordered structure for certain atomic positions of the layers designated with the letter *A* in Fig. 2. We guessed that an ordered structure could be obtained if the *a*-axis were doubled. Subsequently, when we investigated the crystal of the holmium compound, we specifically searched for a doubled *a*-axis. It was indeed observed, although the corresponding reflections (with uneven *h* indices) were weak. It is this unit cell with the doubled *a*-axis, given in Tables 1 and 2, that was used for the data collection and the structure determination. Further experimental details and some results of the structure refinement are summarized in Table 2.

The structure was determined and refined using the program package SHELX-97 [9]. Most atomic positions were located on the basis of a Patterson function. The other positions were found by subsequent Fourier syntheses. The structure was refined by a full-matrix least-squares program with atomic scattering factors, corrected for anomalous dispersion, as provided by the program. The weighting scheme reflected the counting statistics, and a parameter correcting for isotropic secondary extinction was optimized as a least-squares variable.

To check for the correct composition we allowed for variable occupancy parameters together with variable displacement parameters while the scale factor was held constant by the software of the program. It turned out that most atomic positions were fully occupied. Notable exceptions were the positions of the Ho1 and Ho3 atoms with occupancy values close to 95%. On the other hand, the difference Fourier syntheses showed residual electron densities (up to 14.3 e/Å^3) at positions with a difference of $\Delta a \sim 0.5$ of the Ho1 and Ho3 positions. A plausible explanation for these results is the presence of misplaced (by $a/2$) *A* layers (Fig. 2). For that reason we subsequently refined the structure with full occupancy of the *B* layers. In addition we introduced misplaced *A* layers which were shifted relative to the correct position of the *A* layer by half of the translation period *a*. The atomic positions of the main ("correct") layer *A* were allowed to vary, while the atomic positions of the misplaced layer *A* were fixed. The occupancy parameters of the main layer *A* and misplaced layer *A* were constrained to each other during these refinements. For the next series of least-squares cycles we added again $x = \frac{1}{2}$ to the positional parameters of the main *A*

Table 1
Lattice parameters of the gallides $R_3Ru_4Ga_{15}$ (R = Y, Tb–Er) with a new orthorhombic structure type[a]

Compound	*a* (pm)	*b* (pm)	*c* (pm)	*V* (nm^3)
$Y_3Ru_4Ga_{15}$	874.4(2)	958.1(2)	1766.4(4)	1.4799
$Tb_3Ru_4Ga_{15}$	873.7(1)	960.0(1)	1769.8(1)	1.4844
$Dy_3Ru_4Ga_{15}$	873.8(1)	958.1(2)	1767.6(3)	1.4798
$Ho_3Ru_4Ga_{15}$	871.7(1)	956.4(1)	1765.9(3)	1.4723
$Er_3Ru_4Ga_{15}$	871.1(2)	954.4(2)	1764.8(4)	1.4672

[a] These lattice parameters were obtained from Guinier powder data. Standard deviations in the place values of the last listed digits are given in parentheses throughout the article.

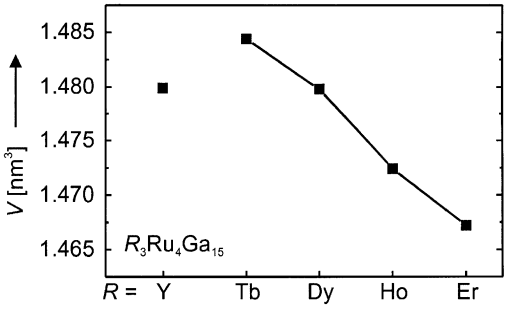

Fig. 1. Cell volumes of the rare earth ruthenium gallides $R_3Ru_4Ga_{15}$ (R = Y, Tb–Er).

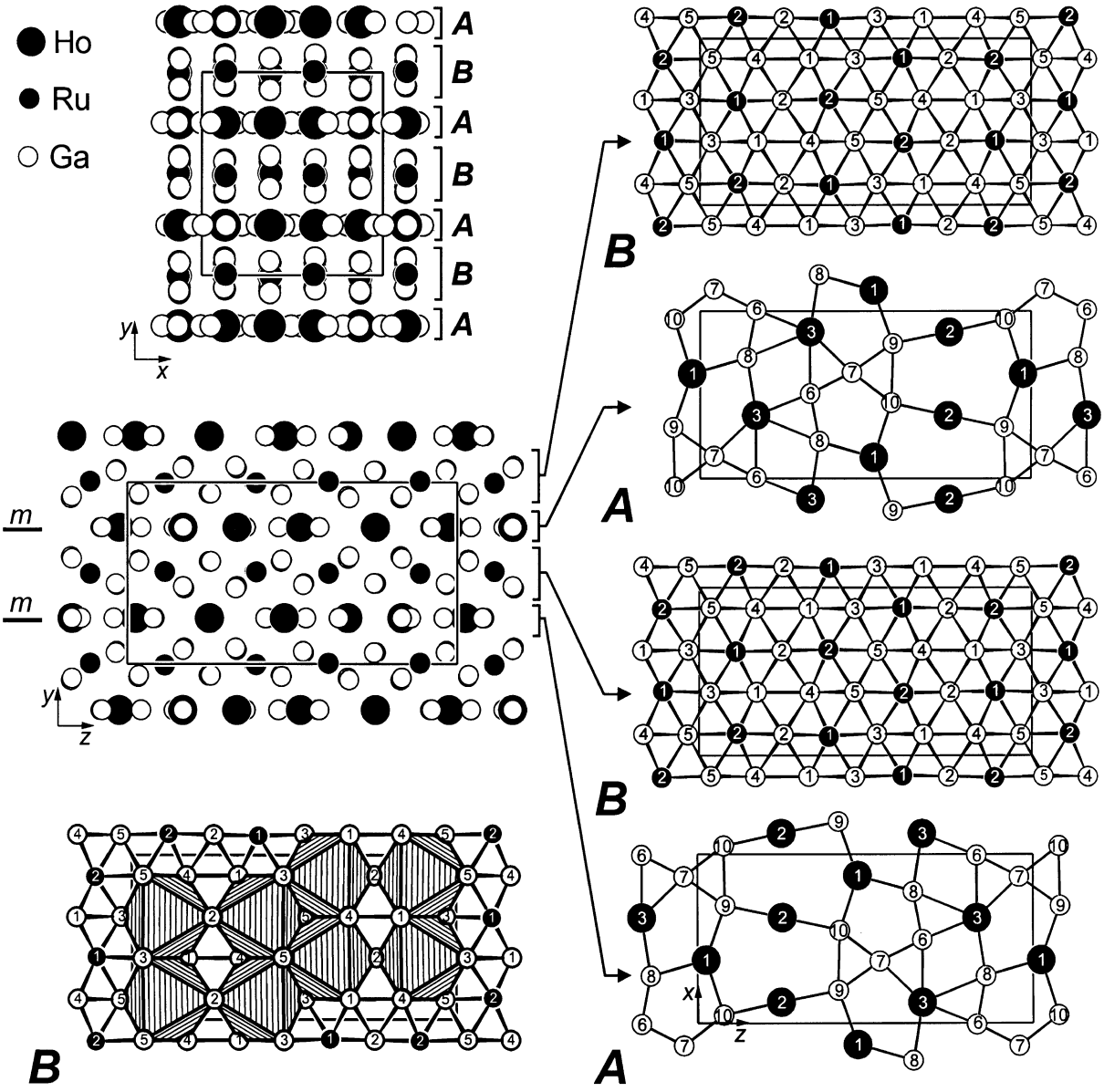

Fig. 2. Crystal structure of $Ho_3Ru_4Ga_{15}$. The numbers correspond to the atom designations. The structure may be considered as containing layers, although chemical bonding within and between the layers is of similar strength. At the left-hand side, in the upper corner and in the middle, two projections of the structure are shown that contain all atoms, mostly superimposed. Certain atomic layers can be discerned. They are shown in the right-hand part of the figure in projections perpendicular to the layers. The layers of the type *A* are situated on mirror planes. Consequently, they are planar. They contain all rare earth and some gallium atoms. The layers of the type *B* consist of puckered hexagonal nets of transition metal and gallium atoms. As is shown for one layer in the lower left-hand part of the figure, these layers may also be viewed as consisting of sheets of condensed edge- and corner-sharing $RuGa_6$ octahedra, which are strongly compressed along the *y* axis.

layer to obtain better positional parameters for the misplaced layers *A*. By this iteration we arrived at the final structure. For the occupancy parameters of the main *A* layer and the misplaced *A* layer we obtained a ratio of 95.0(2)% to 95.0(2)%. The two highest peaks in the final difference Fourier syntheses amounted to 8.2 and 5.3 e/Å^3. They are located within 150 pm of the Ho3, Ga6, and Ga8 positions. We concluded that the refinement with the assumption of misplaced layers was essentially correct. In Tables 3 and 4 we report only the positional parameters and interatomic distances for the main structure. In more detail the results of the structure refinement are deposited. They may be obtained from the Fachinformationszentrum Karlsruhe GmbH, D-76344 Eggenstein-Leopoldshafen, by quoting Registry No. CSD-412472.

4. Discussion

The five ternary gallides $R_3Ru_4Ga_{15}$ (R = Y, Tb–Er) crystallize with a new orthorhombic structure type

Table 2
Crystal data of $Ho_3Ru_4Ga_{15}$

Compound	$Ho_3Ru_4Ga_{15}$
Space group	*Pnma* (No. 62)
Formula units/cell, Z	4
Pearson symbol	*oP*88
Formula mass	1944.9
Lattice constants from Guinier powder [single-crystal] data	
a (pm)	871.7(1) [871.6]
b (pm)	956.4(1) [956.1]
c (pm)	1765.9(3) [1764.8]
V (nm^3)	1.4723 [1.4707]
Calculated density (g/cm^3)	8.77
Crystal size (μm)	$30 \times 30 \times 70$
Scans up to 2θ	60°
Range in h, k, l	±12, ±13, −12 to 20
Ratio highest/lowest transmission	1.91
Total number of reflections	15,730
Internal residual, R_i (I)	0.102
Unique reflections	2130
Reflections with $I_o > 2\sigma(I_o)$	1039
Number of variables	114
Highest/lowest residual electron density ($e/Å^3$)	8.2/−8.0
Conventional residual, R ($F > 2\sigma$)	0.040
Weighted residual, R_w (all F^2 values)	0.177

Table 3
Atomic parameters of $Ho_3Ru_4Ga_{15}$[a]

Atom	*Pnma*	x	y	Z	U_{eq}
Ho1	4*c*	0.1258(2)	$\frac{1}{4}$	0.52487(8)	69(3)
Ho2	4*c*	0.3752(2)	$\frac{1}{4}$	0.74828(8)	52(3)
Ho3	4*c*	0.3759(2)	$\frac{1}{4}$	0.16830(8)	59(3)
Ru1	8*d*	0.1181(2)	0.0040(1)	0.39028(9)	41(3)
Ru2	8*d*	0.1303(2)	0.0050(1)	0.11318(8)	34(3)
Ga1	8*d*	0.1244(3)	0.0869(2)	0.6719(1)	59(4)
Ga2	8*d*	0.1265(4)	0.0609(2)	0.2528(1)	72(4)
Ga3	8*d*	0.3737(3)	0.0684(2)	0.0330(1)	59(4)
Ga4	8*d*	0.3744(3)	0.5774(2)	0.3315(1)	70(4)
Ga5	8*d*	0.3775(3)	0.0616(2)	0.4652(1)	73(4)
Ga6	4*c*	0.0075(4)	$\frac{1}{4}$	0.1684(2)	113(7)
Ga7	4*c*	0.1325(4)	$\frac{1}{4}$	0.0417(2)	68(6)
Ga8	4*c*	0.2218(4)	$\frac{1}{4}$	0.3588(2)	131(7)
Ga9	4*c*	0.3044(4)	$\frac{1}{4}$	0.9184(2)	75(7)
Ga10	4*c*	0.4512(4)	$\frac{1}{4}$	0.5775(2)	74(7)

[a] The structure was refined with anisotropic displacement parameters for all atoms. The last column contains the equivalent isotropic U values (pm^2). The positional parameters were standardized using the program STRUCTURE TIDY [10].

which we have determined for the holmium compound. The large holmium atoms occupy three atomic sites (Fig. 3), all with high coordination numbers (*CN*) of 16 (Ho2) and 17 (Ho1 and Ho3), respectively. They have only gallium and ruthenium neighbors. The Ho–Ga distances cover the relatively narrow range between 295.3 pm (Ho3–Ga3) and 322.3 pm (Ho3–Ga1), with only one exception (Ho3–Ga8: 362.2 pm). The Ho–Ru distances are much greater; they extend between 332.0 pm (Ho3–Ru2) and 359.2 pm). (Ho1–Ru2), even though the gallium atoms with a "metallic" radius (for *CN* 12) of 141.1 pm are larger than the ruthenium atoms with $r = 133.9$ pm [11,12]. This indicates that the Ho–Ga bonding is stronger than the Ho–Ru bonding. The average *R*–Ga and *R*–Ru distances in $Dy_2Ru_3Ga_9$ [1] and $Yb_2Ru_3Ga_{10}$[3] show the corresponding relationship.

They are only two ruthenium positions, both with very distorted icosahedral coordination (*CN* 12) and no Ru–Ru interactions. The Ru–Ga distances vary between 248.9 and 275.5 pm, with averages of 258.1 and 262.5 pm for the Ru1 and Ru2 atoms, respectively. Both are considerably shorter than the sum of the *CN* 12 radii of 275.0 pm.

The gallium atoms occupy 10 atomic sites with between 12 and 15 neighbors of which there are between 1 and 4 holmium atoms, 2 or 3 ruthenium atoms, and between 6 and 11 gallium atoms. The Ga–Ga distances almost continuously cover the very wide range from 249.0 pm (Ga6–Ga7) to 365.0 pm (Gal–Ga10). In this context we remind the reader that the structure of elemental gallium itself is very unusual and irregular, with seven near neighbors for each gallium atom. Of these, 6 gallium atoms are at distances between 270.0 and 279.2 pm and one Ga–Ga distance is very short with 246.5 pm; there are no further Ga–Ga interactions in this structure up to ca. 375 pm [11,13].

We have already pointed out that the structure of $Ho_3Ru_4Ga_{15}$ may be viewed as consisting of atomic layers, even though chemical bonding within the layers and between the layers is of similar strength and character, as can be judged by looking at the near-neighbor coordinations (Fig. 3). The layers of the type *A* (Fig. 2) contain all of the holmium atoms and, in addition, some gallium atoms. These layers correspond to mirror planes of the space group and consequently they are completely flat. Inbetween the layers *A* there are layers we have designated with the letter *B*. The layers *B* contain all of the ruthenium and the remaining gallium atoms. These layers are slightly puckered. The ruthenium atoms are situated on a plane in the middle of these layers, while the gallium atoms are somewhat above and below the ruthenium plane. Alternatively, the layers of the type *B* may be viewed as consisting of infinite sheets of edge- and corner-sharing $RuGa_6$ octahedra which are extremely compressed in the direction perpendicular to the layers, as is outlined in the lower left-hand part of Fig. 2. Four layers are needed to complete one translation period, resulting in the stacking sequence *ABAB*, *ABAB*.

In Table 5 we give a summary of crystal structures which have a layered topology, as just described for the

Table 4
Interatomic distances in the structure of $Ho_3Ru_4Ga_{15}$[a]

Ho1:	Ga9	297.5		Ga8	258.1		Ga10	365.0		Ho2	307.9		2Ga5	286.4
	2Ga3	298.1		Ga4	258.3	Ga2:	Ru1	248.9		Ho2	310.1		Ho3	308.2
	Ga10	298.5		Ga3	259.9		Ru2	252.3		Ga4	330.2		2Ga5	327.3
	2Ga1	302.8		Ga3	261.5		Ga6	256.3		Ga6	333.9	Ga8:	Ga6	253.6
	2Ga5	302.9		Ga5	267.7		Ga8	273.2		Ga8	343.6		2Ru1	258.1
	2Ga3	304.9		Ho3	332.6		Ga4	289.0	Ga5:	Ru2	265.8		2Ga2	273.2
	Ga8	305.0		Ho1	334.5		Ga1	292.5		Ru1	267.7		2Ga5	293.6
	2Ru1	334.5		Ho2	349.2		Ga1	295.9		Ru2	269.1		Ho1	305.0
	2Ru1	355.9		Ho1	355.9		Ga4	296.6		Ga4	270.9		Ho3	305.4
	2Ru2	359.2	Ru2:	Ga2	252.3		Ho2	297.5		Ga5	273.1		2Ga4	343.6
Ho2:	2Ga2	297.5		Ga1	253.4		Ho3	316.0		Ga10	275.5		Ho3	362.2
	2Ga1	300.5		Ga4	256.0		Ho3	319.7		Ga3	278.9	Ga9:	2Ru1	257.0
	2Ga1	302.3		Ga10	261.7		Ga2	361.7		Ga7	286.4		Ga7	264.3
	Ga9	306.7		Ga3	262.2	Ga3:	Rul	259.9		Ga8	293.6		2Ga3	273.5
	2Ga4	307.9		Ga5	265.8		Rul	261.5		Ho1	302.9		2Ga4	274.0
	Ga10	308.8		Ga7	266.2		Ru2	262.2		Ga6	317.7		Ho1	297.5
	2Ga4	310.1		Ga5	269.1		Ga7	273.1		Ga7	327.3		Ho2	306.7
	2Ru2	341.2		Ga6	275.5		Ga9	273.5		Ga10	341.8		Ga10	308.1
	2Ru1	349.2		Ho3	332.0		Ga5	278.9		Ga9	347.6		2Ga5	347.6
Ho3:	2Ga3	295.3		Ho2	341.2		Ga3	281.5		Ga5	360.3		2Ga1	357.1
	Ga8	305.4		Ho1	359.2		Ga1	286.7	Ga6:	Ga7	249.0	Ga10:	2Ru2	261.7
	Ga7	308.2	Ga1:	Ru2	253.3		Ho3	295.3		Ga8	253.6		Ga7	263.2
	Ga6	310.3		Ru1	253.6		Ho1	298.1		2Ga2	256.3		2Ga5	275.5
	2Ga2	316.0		Ga4	282.1		Ho1	304.9		2Ru2	275.5		2Ga4	276.1
	2Ga2	319.7		Ga3	286.7		Ga3	347.3		Ho3	310.3		Ho1	298.5
	Ga6	321.1		Ga2	292.5	Ga4:	Ru2	256.0		2Ga5	317.7		Ga9	308.1
	2Ga1	322.3		Ga2	295.9		Ru1	258.3		Ho3	321.1		Ho2	308.8
	2Ru2	332.0		Ho2	300.5		Ga5	270.9		2Ga4	333.9		2Ga5	341.8
	2Ru1	332.6		Ho2	302.4		Ga9	274.0	Ga7:	Ga6	249.0		2Ga1	365.0
	Ga8	362.2		Ho1	302.8		Ga10	276.1		Ga10	263.3			
Ru1:	Ga2	248.9		Ga1	311.9		Ga1	282.1		Ga9	264.3			
	Ga1	253.6		Ho3	322.3		Ga2	289.0		2Ru2	266.2			
	Ga9	257.0		Ga9	357.1		Ga2	296.6		2Ga3	273.1			

[a] All distances < 380 pm are listed. They were calculated with the lattice parameters from the Guinier powder data. The standard deviations are all equal or less than 0.2 pm.

Table 5
Topology of some related layered crystal structures of intermetallics $R_xT_yM_z$ with a high content of the M component[a]

Structure type $R_xT_yM_z$	Literature	Ratio $(xR+yT)/zM$	Space group	Z	Pearson code	Mesh content (mA)	Mesh content (nB)	Stacking sequence in one translation period[b]
$Gd_3Ru_4Al_{12}$	[14,16]	0.5833	$P6_3/mmc$	2	$hP38$	Gd_3Al_4	$4RuAl_2$	$ABAB$
$Y_2Co_3Ga_9$	[2,15]	0.5556	$Cmcm$	4	$oC56$	$2Y_2Ga_3$	$6CoGa_2$	$ABAB$
$Er_4Pt_9Al_{24}$	[15]	0.5417	$P\bar{1}$	1	$aP37$	Er_2Al_3	$3PtAl_2$	$ABBAB'$
$CeOsGa_4$	[5]	0.5	$Pmma$	6	$oP36$	$3CeGa$	$3OsGa_3$	$ABAB$
$Ho_3Ru_4Ga_{15}$	This work	0.4667	$Pnma$	4	$oP88$	$2Ho_3Ga_5$	$4Ru_2Ga_5$	$ABAB$
$CaCr_2Al_{10}$	[17,18]	0.3	$P4/nmm$	4	$tP52$	$2CaAl_4$	$4CrAl_3$	$ABA'B'$
$YbFe_2Al_{10}$	[18–20]	0.3	$Cmcm$	4	$oC52$	$2YbAl_4$	$4FeAl_3$	$ABAB$
$DyRe_2Al_{10}$[d]	[21,22]	0.3	$P\bar{1}$[c]	5	$aP65$	$DyAl_4$	$2ReAl_3$	$ABA'B'\ AB'A'BAB''$
$TbRe_2Al_{10}$	[18]	0.3	$Cmcm$	8	$oC104$	$2TbAl_4$ $4TbAl_4$	$4ReAl_3$ $8ReAl_3$	$ABA'BABA'B\ ABAB$
$LuRe_2Al_{10}$[d]	[20,22]	0.3	$Cmcm$	12	$oC144$	$2LuAl_4$ $6LuAl_4$	$4ReAl_3$ $12ReAl_3$	$ABA'BAB'ABA'BAB'ABAB$

[a] The last three columns contain the unit mesh contents of the layers A and B and the stacking sequences of these layers.

[b] The primed layers A' and B' differ from the unprimed layers A and B in that they contain atoms with different atoms with different atomic sites (Wyckoff positions). For instance, the layers B of $Er_4Pt_9Al_{24}$ contain the atoms Ru(1), Ru(2), Ru(4), Al(1), Al(3), Al(4), Al(6), Al(7), and Al(9), while the layers B' of that structure contain the atoms Ru(3), Ru(5), Al(2), Al(5), and Al(11).

[c] The structures of $DyRe_2Al_{10}$ has been refined in the space group $P\bar{1}$. However, it is probably better described in a space group of higher symmetry [21].

[d] The structures of $TbRe_2Al_{10}$ and $LuRe_2Al_{10}$ may be viewed in two different ways: with small mesh contents they have 8-and 12-layer sequences along the z axes, respectively; with large mesh contents they both have a 4-layer sequence along the x direction [16]. For these structures only the small meshes corresponding to the stacking along the z axes are shown in Fig. 4.

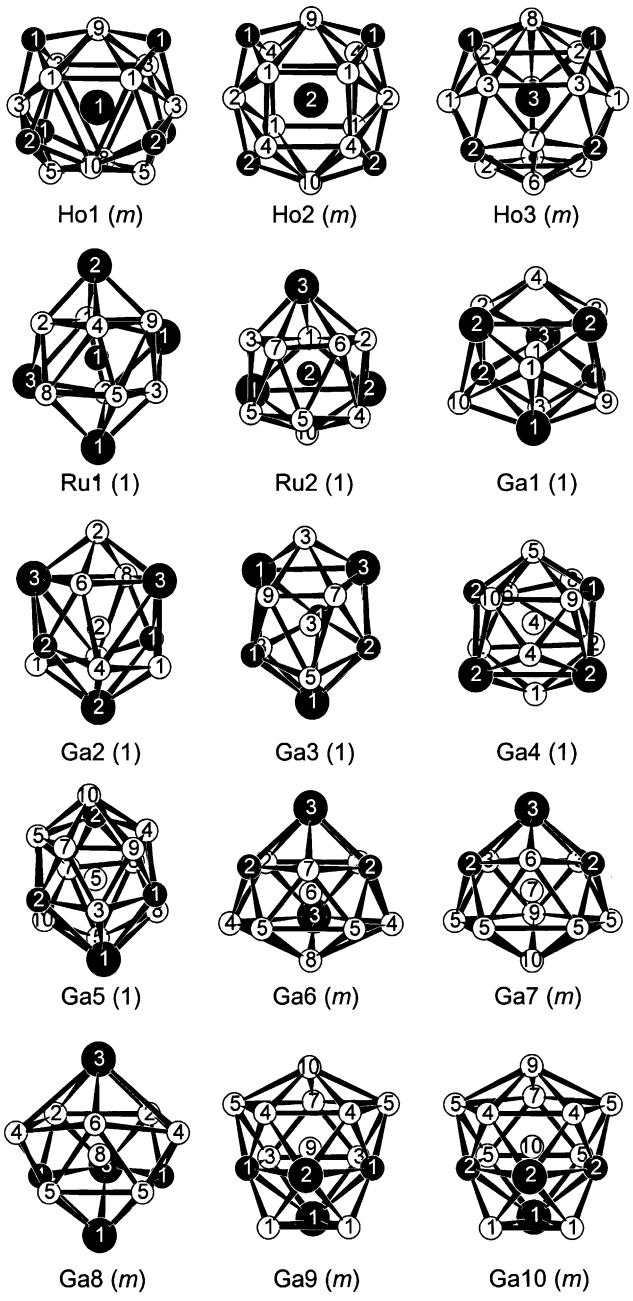

Fig. 3. Near-neighbor environments in the gallide $Ho_3Ru_4Ga_{15}$. All neighbors as listed in Table 4 are shown. Single-digit numbers correspond to the atom designations. The site symmetries are indicated in parentheses.

structure of $Ho_3Ru_4Ga_{15}$. The first column contains the overall composition $R_xT_yM_z$ (R, mostly rare earth elements; T, transition metals; M, main group metals). We have listed the structure types with increasing content of the component M, that is, with decreasing ratio $(xR+yT)/zM$. We also list the space groups, the number of formula units per cell (Z), the Pearson code [23, 24], the content of the unit meshes of the layers A (containing all R atoms and some M atoms), the content of the unit meshes of the layers B (containing all T atoms and some M atoms), and finally the stacking sequence of the layers A and B. Usually, the type A and B layers alternate. However, in the structure of $Er_4Pt_9Al_{24}$, layers of the type B (with the composition $PtAl_2$) are situated also adjacent to each other, resulting in the stacking sequence $ABBAB'$, $ABBAB'$ [15]. In this context it is of interest that the crystal structures of several transition metal aluminides TAl_2 and gallides TGa_2 with $TiSi_2$-, $CrSi_2$-, and $MoSi_2$-type structures [23] consist only of layers of the type B, however, with slightly different interfaces [15, 16, and references therein].

The various layers A and B occurring in the structures of the ternary compounds are shown in Fig. 4. Some of these have already been outlined in previous publications [5, 15, 16, 18, 20, 21]. We should point out that we now have interchanged the letters A and B, with respect to earlier publications, simply because in the formulas of the compounds $R_xT_yM_z$ the R components Ca and the rare earth elements (occurring in the layers A) are listed first, and the transition elements T (situated in the layers B) are listed as the second element. Generally, layers of the type A are flat, frequently as a consequence of space group symmetry, because they usually coincide with mirror planes, as is the case for the structure of $Ho_3Ru_4Ga_{15}$ (Fig. 2). In contrast, layers of the type B are always puckered and the most extreme atomic positions off the plains are always taken by the M atoms, while the transition metal atoms T are located exactly on the plane or very close to it. Layers of the type B may always be considered as consisting of condensed TM_6 octahedra. For the composition TM_2 these octahedra share only edges, while for compositions with $T{:}M<1{:}2$, corner sharing of the octahedra is possible, as demonstrated for $Ho_3Ru_4Ga_{15}$ (with a mesh formula T_2M_5) or the various structures with the composition RT_2M_{10} where the layers B have the formula TM_3 (Fig. 4). We have not thoroughly searched the literature for other structures with a high M content following these building principles. For that reason we expect that several other crystal structures remain to be discovered which can be classified as topologically related to the structures listed in Table 5. This structural family becomes even larger if defect variants are included. For instance, the ordered Th_2Zn_{17}-type structure of the compounds $R_2T_3Zn_{14}$ (T=Fe, Co, Rh, Ni, Pd, Pt) may be viewed as consisting of layers of the composition R_2Zn_6 that alternate with layers of composition T_3Zn_8. The latter layers contain unoccupied sites, voids V, corresponding to the formula VT_3Zn_8 [25]. If these voids were filled by T atoms, these layers would correspond to the B layers TM_2 found in the structures of $Y_2Co_3Ga_9$ and $Er_4Pt_9Al_{24}$ (Fig. 4).

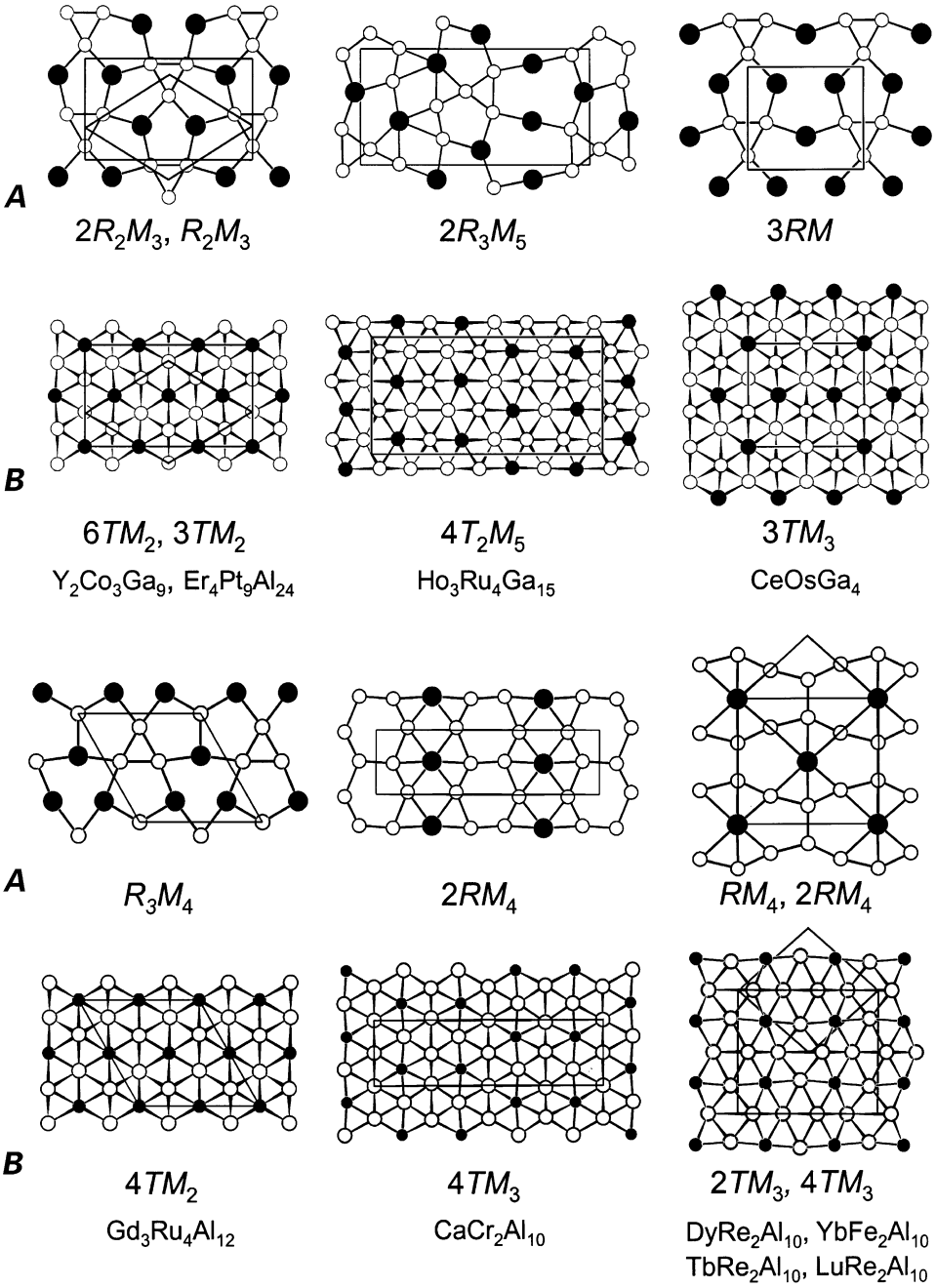

Fig. 4. Atomic arrangements within the various layers *A* and *B* in crystal structures of calcium and rare earth (*R*) transition metal (*T*) main group metal (*M*) intermetallics with the composition $R_xT_yM_z$ and a high content of the *M* component. The layers of the type *A* contain all of the large electropositive atoms *R*; they are flat. The layers *B* are puckered; they contain the late transition metal atoms *T* and additional main group metals *M* (mainly aluminum and gallium). Table 5 may be consulted for more details.

Acknowledgments

We thank Dipl.-Ing. U. Ch. Rodewald for the competent data collection on the four-circle diffractometer and Mr. H.-J. Göcke for the work at the scanning electron microscope. We obtained generous gifts of ruthenium powder, gallium ingots, and silica tubes from Dr. W. Gerhartz (Degussa), Dr. D.J. Braun (VAW), and Dr. G. Höfer (Heraeus Quarzschmelze), respectively. This work was also supported by the Fonds der Chemischen Industrie, the Deutsche Forschungsgemeinschaft, and the International Centre for Diffraction Data.

References

[1] M. Schlüter, W. Jeitschko, Z. Anorg. Allg. Chem. 626 (2000) 2217.

[2] Yu.N. Grin', R.E. Gladyshevskii, O.M. Sichevich, V.E. Zavodnik, Ya.P. Yarmolyuk, I.V. Rozhdestvenskaya, Sov. Phys. Crystallogr. 29 (1984) 528.
[3] M. Schlüter, W. Jeitschko, Inorg. Chem. 40 (2001) 6362.
[4] E. Czech, G. Cordier, H. Schäfer, J. Less-Common Met. 95 (1983) 205.
[5] M. Schlüter, W. Jeitschko, Z. Anorg. Allg. Chem. 628 (2002) 1505.
[6] O.M. Sichevich, V.A. Bruskov, Yu.N. Grin', Sov. Phys. Crystallogr. 34 (1989) 939.
[7] M. Schlüter, W. Jeitschko, 13th International Conference on Solid Compounds of Transition Elements, Stresa, Italy, April 2000.
[8] K. Yvon, W. Jeitschko, E. Parthé, J. Appl. Crystallogr. 10 (1977) 73.
[9] G.M. Sheldrick, SHELX-97, a program package for the solution and refinement of crystal structures, Universität Göttingen, Germany, 1997.
[10] L.M. Gelato, E. Parthé, J. Appl. Crystallogr. 20 (1987) 139.
[11] J. Donohue, The structures of the elements, wiley, New York, 1974.
[12] E. Teatum, K. Gschneidner, J. Waber, LA-2345, US Department of Commerce, Washington, DC, 1960; See W.B. Pearson, The crystal chemistry and physics of metals and alloys, Wiley, New York, 1972.
[13] B.D. Sharma, J. Donohue, Z. Kristallogr. 117 (1962) 293.
[14] R.E. Gladyshevskii, O.R. Strusievicz, K. Cenzual, E. Parthé, Acta Crystallogr. B 49 (1993) 474.
[15] V.M.T. Thiede, B. Fehrmann, W. Jeitschko, Z. Anorg. Allg. Chem. 625 (1999) 1417.
[16] J. Niermann, W. Jeitschko, Z. Anorg. Allg. Chem. 628 (2002) 2549.
[17] G. Cordier, E. Czech, H. Ochmann, H. Schäfer, J. Less-Common Met. 99 (1984) 173.
[18] B. Fehrmann, W. Jeitschko, Z. Naturforsch. B 54 (1999) 1277.
[19] S. Niemann, W. Jeitschko, Z. Kristallogr. 210 (1995) 338.
[20] B. Fehrmann, W. Jeitschko, Inorg. Chem. 38 (1999) 3344.
[21] B. Fehrmann, W. Jeitschko, unpublished results, 1999.
[22] B. Fehrmann, Darstellung und Charakterisierung von Aluminiden und Silico-Phosphiden der Seltenerd- und Übergangsmetalle, doctoral thesis, Münster, 1999.
[23] P. Villars, L.D. Calvert, Pearson's handbook of crystallographic data for intermetallic phases, 2nd ed., Am. Society for Materials International, Materials Park, OH, 1991.
[24] E. Parthé, L. Gelato, B. Cabot, M. Penco, K. Cenzual, R.E. Gladyshevskii, TYPIX, standardized data and crystal chemical characterization of inorganic structure types, Gmelin handbook of inorganic and organometallic chemistry, Vols. 1–4, Springer, Berlin, 1994.
[25] N. Gross, G. Block, W. Jeitschko, Chem. Mater., in press.